

# Recent Advancements in Aerothermodynamic Design Optimization of Spiked hypersonic Winged Re-Entry Vehicle using CFD

P. Harish  
PG Student

Dept. of Mechanical Engineering  
K.S.R.M College of Engineering  
Kadapa, Andhra Pradesh-516003.

Naveen. HN

Research Assistant

High Speed Wind Tunnel complex  
Dept. of Aerospace Engineering  
Indian Institute of Science, Bangalore-12

Dr. K Rajagopal  
Professor. & HOD

Dept. of Mechanical Engineering  
K. S. R. M College of Engineering  
Kadapa, Andhra Pradesh-516003

**Abstract**—During the conceptual design of a Aerospikes in a re-entry vehicle, the spikes shape and geometry is varied and its impact on performance is evaluated, In this study, the shape optimization of two classes of spikes has been studied: A spike with tip as slender & blunt. On one hand, sharp slender spike design reduces the drag and ensures long ranges and more economic flights. However they are more vulnerable to aerodynamic heating. On the other hand, blunt spike produce more drag. However, they are preferred as aeroheating is concerned. In addition, in the content of hypersonic winged vehicles, blunt spike geometries are preferred over slender ones for practical implications such as higher volumetric efficiency, better accommodation of crew or on board equipment. Also, it is found that imposing pitch-stability for the winged vehicle at all angle of attacks results in spike shapes which require upward control surface deflections during the majority of the entry. These spikes are placed in front of the nose region to avoid stronger shocks for reducing the temperature at the nose. Cad Model was created in solid works, meshing in Gambit 2.4.6 & post processing using FLUENT 6.3.

**Keywords:** Aerothermodynamics, spike, heat flux; heat transfer co efficient.

## 1. INTRODUCTION

Hypersonic vehicles experience high levels of drag and aerodynamic heating during flight. Many efforts are devoted to minimizing these effects for longer ranges, lower fuel consumption, and safer flights. One approach is to use spikes. A spike is a needle-like body mounted at the nose tip of the main blunt body. The basic mechanism of drag and heating reduction is twofold: first, replacing the strong detached bow shock ahead of the blunt body by a much weaker oblique foreshock; second, encouraging separation of the flow downstream of the foreshock and creating a recirculation zone that screens a large portion of the main body nose surface. Fig. 1 illustrates this mechanism. The shear layer that envelopes the recirculation zone reattaches on the main body surface and a shock wave, called the reattachment shock, is created to turn the outer flow at the body shoulder.

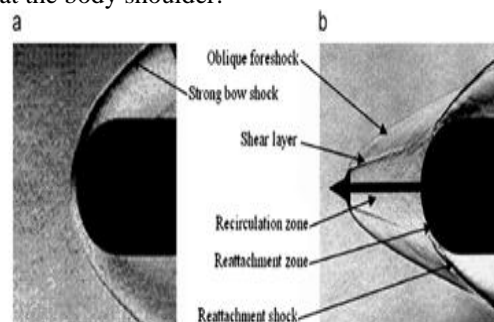


Fig. 1. Macroscopic features of the flowfield ahead of a blunt forebody in hypersonic speeds. (a) without [23] and (b) with the spike/aerodisk [4].

Thus, it was believed that the heating loads can be reduced by altering the flow field pattern ahead of the blunt body so as to replace it with a weaker system of shock waves. A variety of designs are considered. These designs include spikes and aero disks, and even supersonic projectiles fired

ahead of the blunt forebody. Out of these varieties of techniques, the use of spikes proved to be the simplest and the most effective technique in reducing aerodynamic heating.

## 2. GEOMETRY AND GRID

The 2D cad geometry was developed using solid works cad software as shown in fig 2.1

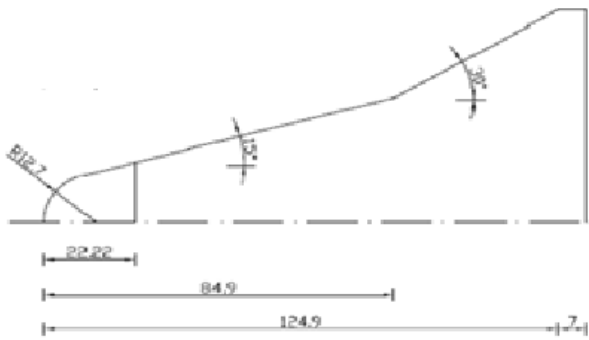


Fig2.1 shows the 2D geometry of the hypersonic winged re-entry vehicle (without Spike).

A spike of two designs was introduced at the nose region of hypersonic winged re-entry vehicle. Blunt spike with entire length 40mm and having radius of 3mm as shown in fig 2.2. Slender spike of length 40 mm and having slender angle of  $17.06^\circ$  as shown in fig 2.3.

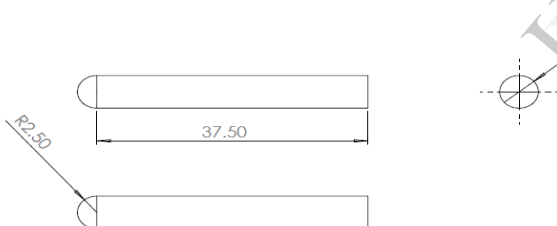


Fig 2.2 shows the 2D geometry of Blunt spike

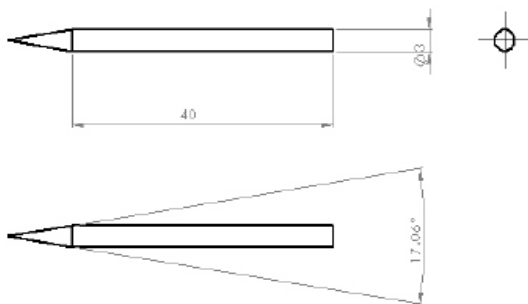


Fig 2.3 shows the 2D geometry of slender spike

Both the cad geometries of without spike and with spike (Blunt & Slender spike) was imported to the gambit software in the igs format .and generated the mesh as shown in the fig 2.4, 2.5.1 & 2.5.2

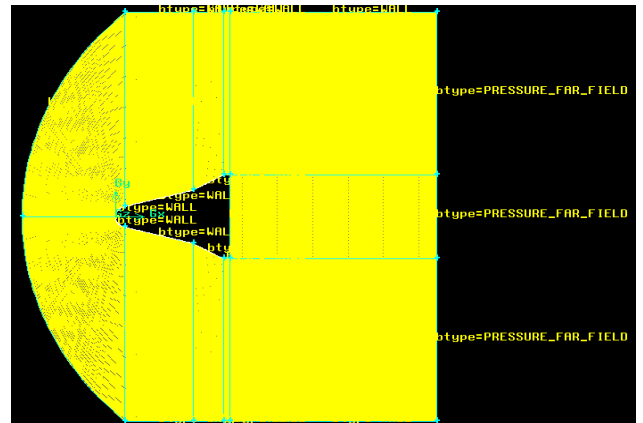


Fig 2.4: without spike meshed and boundary conditions

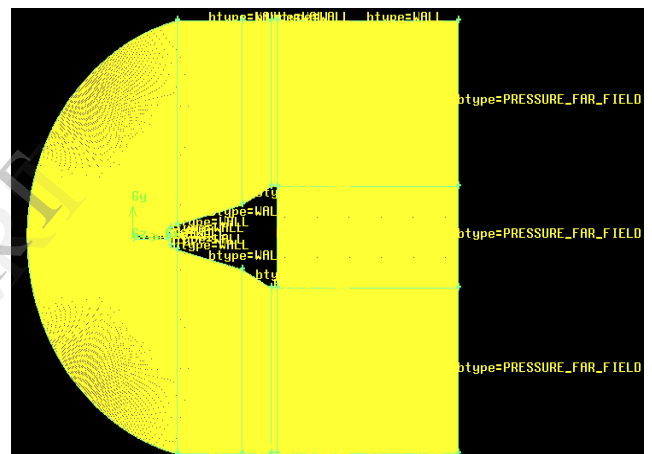


Fig 2.5.1: with Blunt spike meshed and boundary conditions

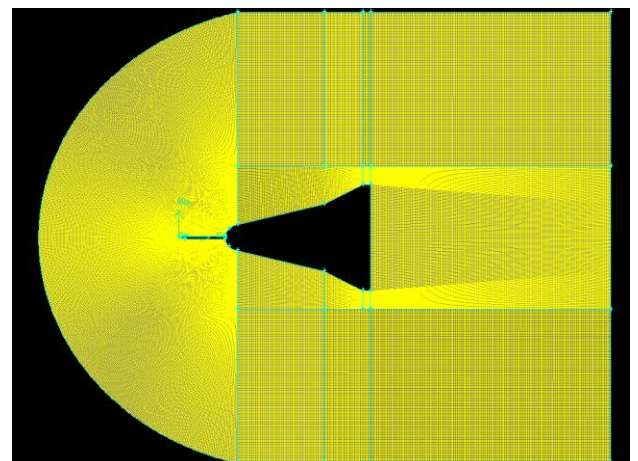


Fig 2.5.2: with slender spike meshed and boundary conditions

The grids were made very fine at the surfaces and coarse as it goes away from the body. Domain extending from 1.5L major length of the model at the face and 2.5L times behind the geometry and 2l of the top and bottom of the geometry model Pressure inlet condition was set to the inlet of the meshed model where inlet pressure are specified and pressure far field was set to the pressure outlet and top and bottom of model and body was set to the wall boundary condition.

2.1 BOUNDARY CONDITIONS

The flow conditions that was used in this analysis is shown in the below table.

Inlet	50 bar
Outlet	0.0022025 bar
Body	Wall
Temperature	773k
Mach No	9.1

The CFD analysis was conducted for density based implicit formulation 2D Flow, the compressible flow is coupled to the energy equation for the flow simulation using Spalart-Allmaras Model.

3. RESULTS & DISCUSSIONS

3.1 Experimental Results:

The experiment was done at Delft University of Technology, Netherlands .The tunnel was operated at a free stream of Mach number 9.1. The settling chamber of the wind tunnel is pressurized at a total pressure P<sub>0</sub> ranging between 25 and 75 bars. The fluid (dry air) is heated to a stagnation temperature of 773 K with a temperature controlled electrical heating system.

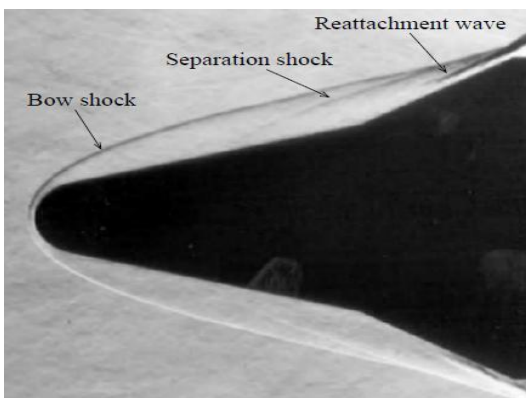


Fig 3.1.1 shows Schlieren image from the high speed Camera for a nose experiment at free M<sub>∞</sub> = 9.1.

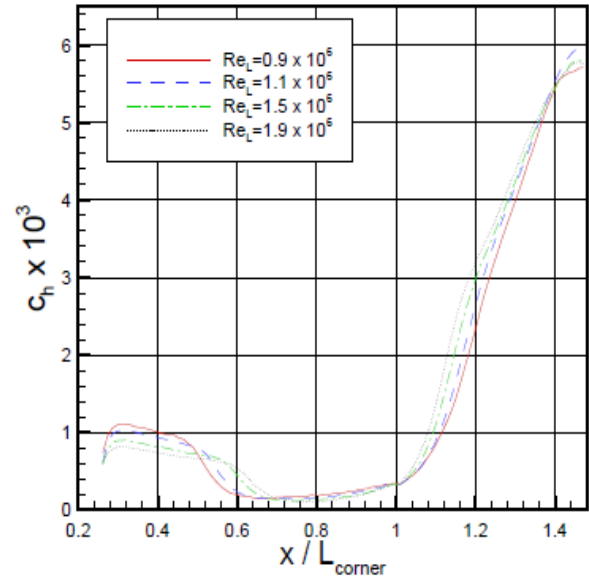


Fig.3.1.2 shows the heat transfer for the experimental model at different Reynolds number with free stream M<sub>∞</sub> =9.1

3.2. CFD Results:

3.2.a Temperature contour plots for without spike configuration

From the temperature contour we observe that temperature is maximum at nose of the blunt body for without spike model, the bow shock temperature near the nose is observed to be 900K. This shock wave scatter the heat into the flow field so temperature decreases along the body as seen in the fig 3.2.1

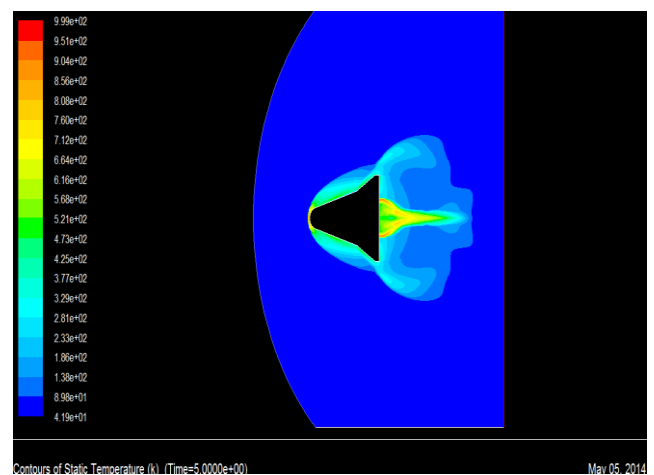


Fig 3.2.1: Temperature profile of without spike at 50 bar

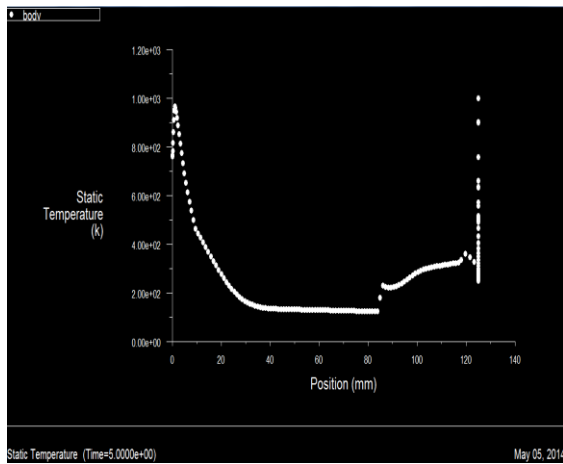


Fig 3.2.2 shows variation of temperature vs length for without spike model.

3.2.b Temperature contour plots of with spike(Blunt) configuration.

As the introduction of the Blunt spike at the nose of the blunt body we observed that the temperature at the nose was 625 k. The shock wave scattered along the length and decreases the temperature along physical domain.

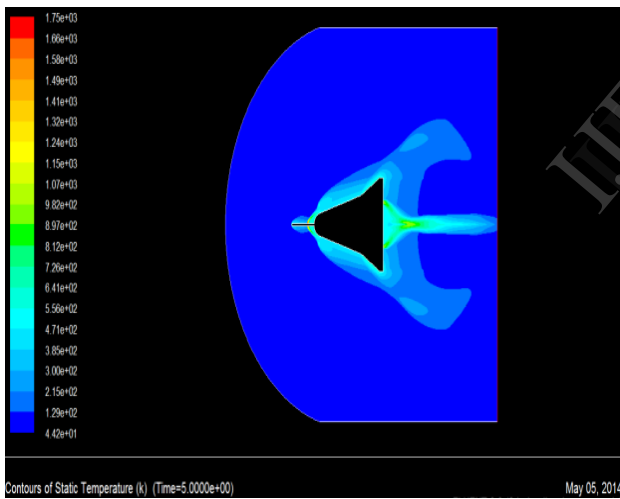


Fig .3.3.1: Temperature Profile of with spike (Blunt) configuration at 50 bar

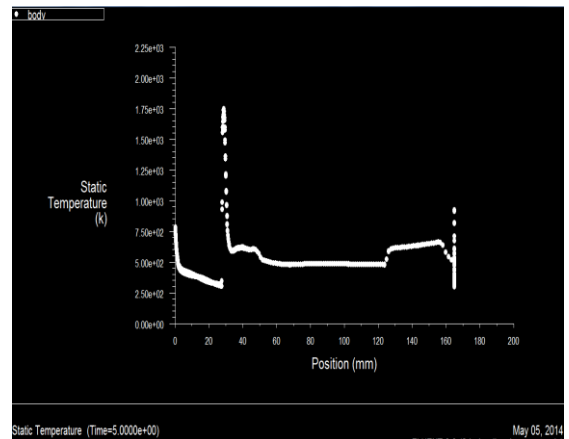


Fig 3.3.2: shows variation of temperature vs length for the Blunt spike model.

3.2.c Temperature contour plots of with spike (Slender) configuration.

As the introduction of the slender spike at the nose of the blunt body we observed that the temperature at the nose was around 800 k. The shock wave scattered along the length and decreases the temperature along physical domain

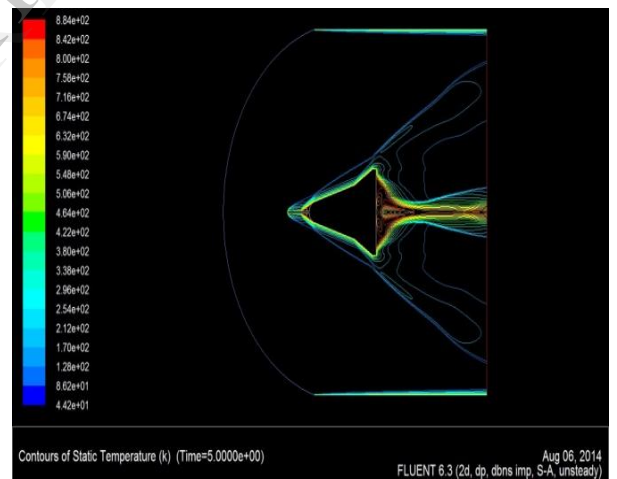


Fig .3.4.1: Temperature Profile of with spike (Blunt) configuration at 50 bar

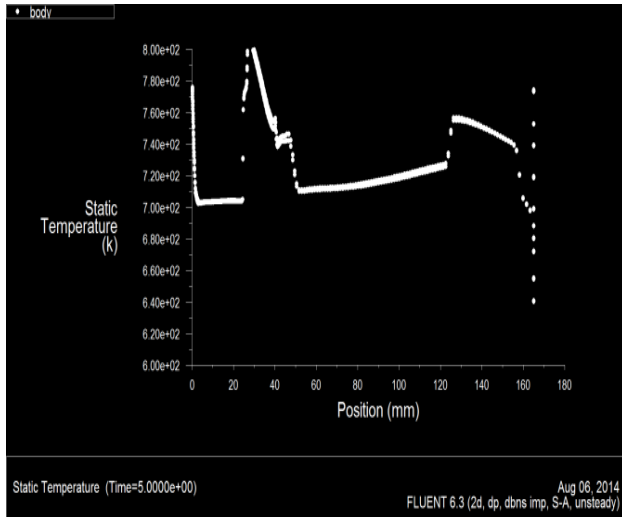


Fig 3.4.2: shows variation of temperature vs length for the Slender spike model.

3.2.d Calculation of Heat Transfer Co-efficient( $C_H$ ):

The Heat Transfer Rate is given by the relation

$$q = \rho c l (dT/dt) \dots\dots\dots 1$$

Where the values of  $\rho$  (density),  $c$ (specific heat) and  $l$ (thickness) of the skin are

' $\rho$ ' density of Stainless Steel = 8000 Kg/m<sup>3</sup>

' $c$ ' specific heat of Stainless Steel = 502 J/Kg K

' $l$ ', thickness of the material = 1.0 mm

and the co-efficient of heat transfer is calculated by using the equation(2)

$$C_H = \frac{q}{\rho_{\infty} C_{p_{\infty}} U_{\infty} (T_o - T_w)} \dots\dots\dots 2$$

Where,  $\rho_{\infty}$ ,  $U_{\infty}$ , and  $C_{p_{\infty}}$  are free-stream density, velocity and specific heat at constant pressure.  $T_o$  is stagnation temperature of the given run and  $T_w$  is wall temperature at a given instant time.

3.3 Comparison of Experimental Result with CFD results :

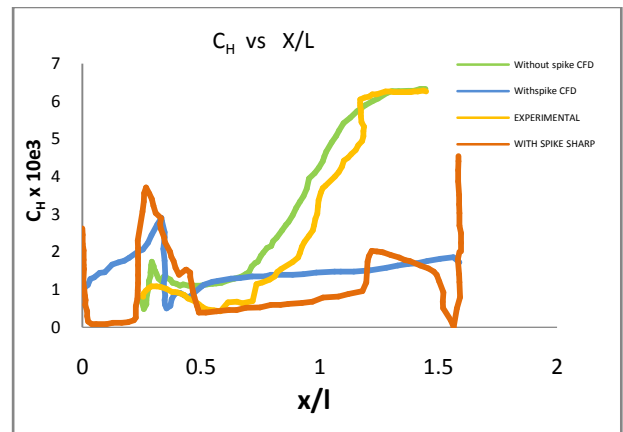


Fig 3.5: Shows the Variation of  $C_H$  with length at free stream Mach Number  $M_{\infty}=9.1$ .

The above graph shows the variation of  $C_H$  with respect to length for both experimental and CFD result. As we notice that by introducing the Blunt spike to the model there is 30.5% reduction of heat at the nose of the model, and for slender spike it is around 11.5%.

From the above graph we can notice that slender spike heat reduction at nose is comparatively less, but at the body is high. When the slender spiked vehicles are good is compared with without spiked vehicles. But the Blunt spiked vehicles are comparatively good over slender ones.

4. CONCLUSION

In spite of the decades of research into hypersonic flow; there are still many challenges to analyzing and designing high-speed vehicles. Recent events such as the Columbia accident are clear evidence that there are still "unknown unknowns" in the field of hypersonic flight that even our best experimental or numerical analysis cannot adequately predict.

While analyzing both with spiked (Blunt & Slender) hypersonic vehicle the temperature of the Blunt spiked vehicle reduces at the nose compared to Slender, due to reduction in the bow shock wave and also pressure of the nose vehicle so that there is less possibility or more time to take disaster of the hypersonic re-entry vehicles.

## 5. SCOPE OF FUTURE WORK

Introduction of spike in hypersonic vehicles are there. Since work have been going in the hypersonic vehicle. very few people are doing work on introducing spike on the hypersonic re-entry vehicle . Since No static temperature data exists for Mach number in the range 8-14. Also data on large nose radius do not exist.

Keeping in view of future requirements in the country as well as to generate data base towards extending some of existing static temperature ,correlations , a detailed CFD study of hypersonic laminar surface flows on several spiked models this will have relevance to reentry missions

## 6. REFERENCES

- [1]. Ferry F.J. Schrijer and Fulvio Scarano and Bas W. van Oudheusden was conducted on experiment on Hypersonic Boundary Layer Separation and Reattachment on a Blunted Cone-Flare using Quantitative Infrared Thermography 2003.
- [2]. Antonio Viviani and Giuseppe Pezzella was studied Heat Transfer Analysis for a Winged Reentry Flight Test Bed 2005.
- [3]. M.Y.M. Ahmeda N. Qin investigated Recent advances in the aerothermodynamics of spiked hypersonic vehicles 2011
- [4]. Zonglin Jiang and Yunfeng Liu and Guilai Han was conducted on In order to achieve efficient wave drag reduction under non-zero attack angles and avoid the severe aerodynamic heating, a new concept of the Non-ablative Thermal Protection System (NATPS) for hypersonic vehicles. 2011.
- [5]. N.Sreenivasa Babu. Dr. K. Jayathirtha Raowas studied Aerodynamic drag and heating are the crucial in the thermal stability of hypersonic vehicles at various speeds.
- [6]. Agosh M C had conducted on experiment Aerodynamic and Heat Transfer Analysis over Spherical Blunt Cone.
- [7]. D. Dirx, E. Mooij Delft University of Technology, Faculty of Aerospace Engineering, Section of Aerodynamics and Space Missions, Kluyverweg
- [8]. D. Kinney, Aerodynamic Shape Optimization of Hypersonic Vehicles, 44th AIAA Aerospace Sciences Meeting and Exhibit, No. AIAA 2006- 239, 2006.

IJERT